Ultrathin transition-metal dichalcogenides and 2D optoelectronics

A strong coupling of light and electrons and holes in ultrathin transition-metal dichalcogenides has opened prospects for efficient solar cells. Mike Cooke reports on developments in devices and structures consisting of compounds of the transition metals molybdenum (Mo) and tungsten (W) and the chalcogenides sulfur (S) and selenium (Se).

Transition-metal dichalcogenides (variously abbreviated as MX_2, TMD, TMDC) have become the trendy research vehicle for ultrathin two-dimensional (2D) electronics. With an eye to funding, researchers can often make exaggerated and/or misleading claims about their results and this is particularly true in new areas of study such as this. Similar claims were made in the early days of graphene research, and we can expect a sequence of optimism, pessimism and, finally, realism for both graphene and now TMDs. While we do our best here to find solid results and paths to real applications rather than wishful thinking, errors made in this respect are inevitable.

The crystal structure of TMD materials consists of strong bonds within a plane and weaker van der Waals bonds between layers. Like graphene, a 'facile' exfoliation technique to create flakes of a few layers, or even monolayers, of TMD materials is to use Scotch tape. By simply sticking the tape on bulk material and pealing it off, one can carry away flakes that are then removed from the tape and studied under a microscope or floated in solution onto a substrate. Although exfoliation is indeed 'facile', in the sense of being simple to implement, it is very labor intensive and could not lead to a robust mass-production process.

Much of the interest for TMD devices centers on the large optical coupling to direct-bandgap transitions leading to photovoltaic possibilities. Direct bandgaps are needed for efficient optoelectronics. The bandgap is around 2eV, a region of particular interest for solar cells. Although the bare efficiencies are small, it has to be remembered that these are responses for a few atomic layers (~0.3nm per TMD layer), whereas standard solar cells have micron-scale absorber layers. Another feature is that the electron–hole binding into excitons is large at around 0.5eV. Excitons appear in photoluminescence studies as resonance peaks and usually couple strongly to incoming photons.

Ultrafast charge separation

For solar cells one needs the electrons and holes generated by incoming photons to separate and thus produce a current, rather than recombining. Researchers in the USA and China have demonstrated "for the first time" efficient electron–hole separation through charge transfer in molybdenum/tungsten disulfide (MoS_2/WS_2) monolayer semiconductor heterostructures [Xiaoping Hong et al, Nature Nanotechnology, published online 24 August 2014].

The researchers from University of California at Berkeley, Lawrence Berkeley National Laboratory, Peking University, Arizona State University, and Kavli Energy NanoSciences Institute, say that the hole transfer time from the MoS_2 to WS_2 layer is ultrafast, at less than 50 femtoseconds ($50x10^{-15}$ seconds or, more correctly, $5x10^{-14}$ seconds). While the hole transfers to the WS_2 layer, the electron remains behind in the MoS_2.

Beyond solar cells, the researchers also see opportunities for photodetection, photovoltaics and photocatalysis arising from the combination of the demonstrated ultrafast charge transfer and strong optical absorption of MX_2 semiconductors.

The researchers chose to study the MoS_2/WS_2 combination because previous theoretical work suggested that these materials would form a 'type II' band profile, with the conduction band lowest in one material and the valence band highest in the other (Figure 1). With such an energy-level structure, the electrons would congregate in the material with the lowest conduction band and the holes in the material with the highest valence band (holes 'float' upwards in energy), hopefully enabling efficient separation for energy harvesting.

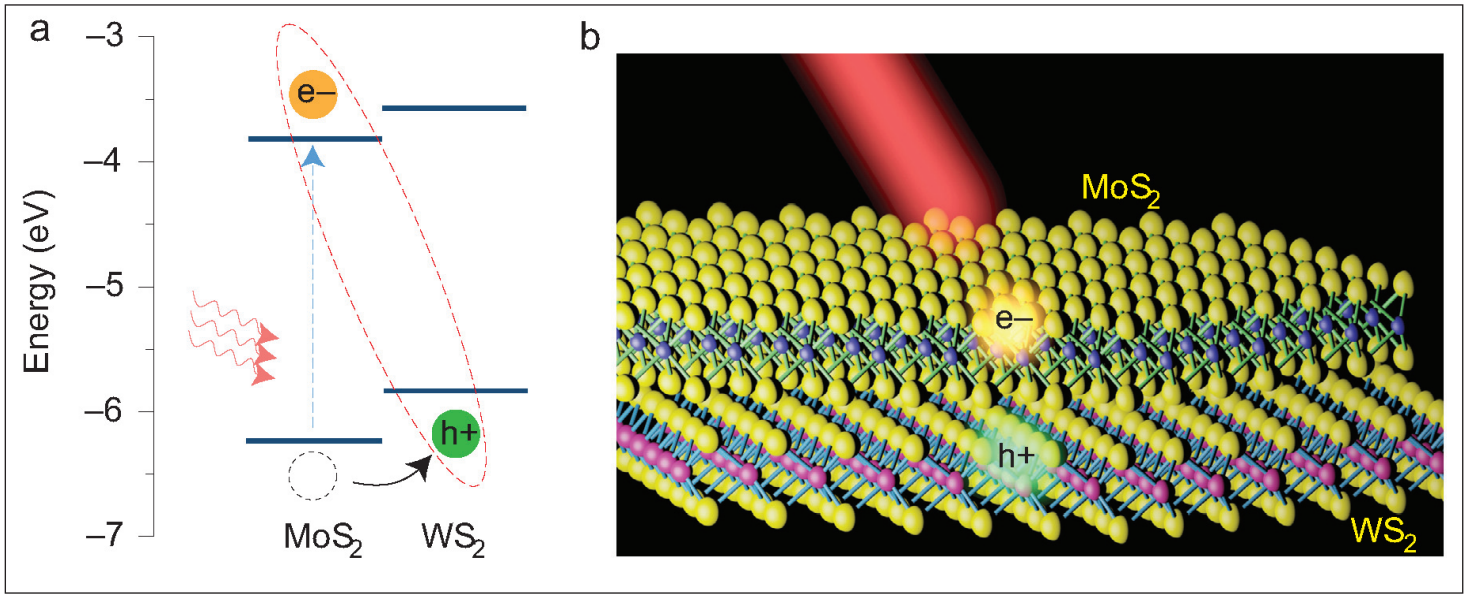

Figure 1. Band alignment and structure of MoS_2/WS_2 heterostructures. (a) Schematic of theoretically predicted band alignment of MoS_2/WS_2 heterostructure. (b) Illumination of MoS_2/WS_2 heterostructure with MoS_2 monolayer lying on top of WS_2 monolayer creates electron and hole in separate layers.

The MoS_2 monolayer was grown on 285nm silicon dioxide on silicon substrate, using chemical vapor deposition (CVD). The WS_2 monolayer was grown on sapphire, again with CVD. The WS_2 material appeared on the sapphire substrate as flakes.

The MoS_2 was transferred to the WS_2 on sapphire on polymethyl methacrylate (PMMA) film. The film was spin coated on the MoS_2 and released from the substrate by etching in potassium hydroxide solution. After transfer onto the WS_2, the PMMA was dissolved in acetone.

The MoS_2/WS_2/sapphire was annealed to create the heterostructure. Raman spectroscopy was used to confirm that the heterostructure consisted of monolayers of MoS_2 and WS_2.

Photoluminescence with 2.33eV radiation at 77K on regions with only MoS_2 or WS_2 gave

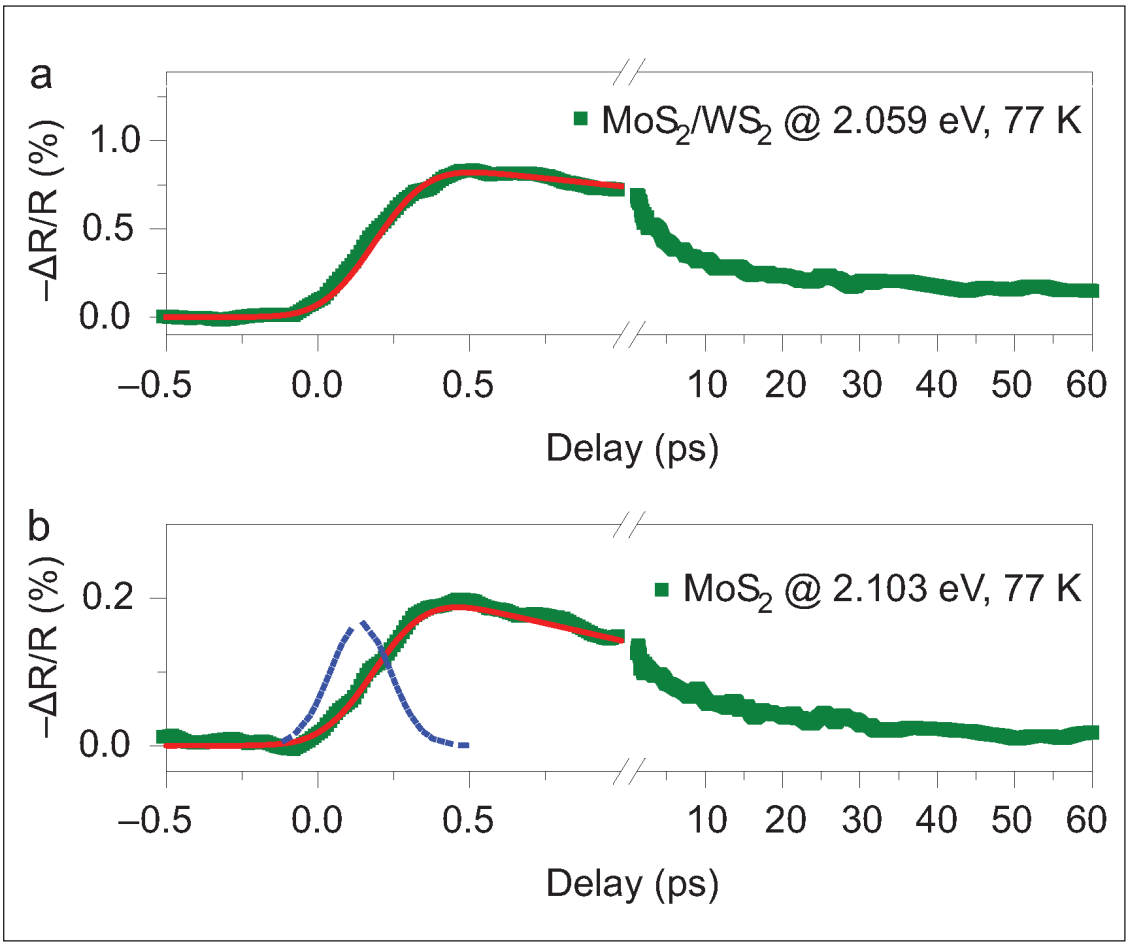

Figure 2. (a) Evolution of transient absorption signals at the WS_2 A-exciton resonance in MoS/WS_2 heterostructure. (b) Dynamic evolution of transient absorption signals at the MoS_2 B-exciton resonance in isolated MoS_2 monolayer. Both signals show almost identical ultrafast rise times, limited by laser pulse duration of ~250fsecs. Convoluting instrument response function (blue dashed line in b) and instantaneous response in MoS_2 reproduces ultrafast dynamics in MoS_2 monolayer (red trace in b). Similar convolution shows that rise time in the MoS_2/WS_2 monolayer is ~25fsecs (red trace in a) and has an upper limit of 50fsecs.

resonance peaks at 1.93eV or 2.06eV, respectively. The researchers attribute these resonances to 'A-excitons'. In regions where MoS_2 overlaid WS_2 to form a hetero-structure, these peaks were significantly 'quenched'. The researchers take this as evidence that charge transfer had taken place with the separation of the electrons and holes into the MoS_2 and WS_2 layers, respectively. An alternative quenching mechanism of energy transfer would by contrast reduce the high-energy peak and enhance the lower-energy peak, according to the researchers. The quenching effect was also seen in room-temperature measurements.

The researchers also carried out more detailed pump-probe experiments at 77K. The probe consisted of detecting changes in the reflection spectrum at various times after the pump pulse. By changing the energy of the pump photons the separate excitons could be generated. The researchers used a 1.86eV photon pump to generate MoS_2 excitons. The change in reflection spectrum was directly proportional to the absorption spectrum.

Resonant features at 2.06eV and 2.46eV were found in the absorption spectra of MoS_2/WS_2 heterostructures. The researchers attribute these, respectively, to the A- and B-exciton states in WS_2. Such features are not seen in WS_2-only samples since the pump energy is too low to excite them. The researchers comment: "This provides direct evidence of efficient charge separation in photoexcited MoS_2/WS_2 heterostructures (Figure 1a): electron–hole pairs are initially created in the MoS_2 layer, but holes quickly transfer to the WS_2 layer due to the type II band alignment, while electrons stay in the MoS_2 layer."

Using the rise time for the exciton resonance, the researchers estimate that the hole transfer occurs within 50fsecs of the pump pulse (Figure 2). "Similar ultrafast hole transfer also takes place at room temperature," the researchers say. Most processes in MX_2 materials, such as exciton lifetimes, are typically on the order of tens of picoseconds (10^{-12} seconds).

The researchers believe that the efficient charge separation is due in part to the formation of 'charge transfer excitons' with the electrons and holes binding across the interface between the different layers.

Vienna University of Technology has similarly created vertical type II structures using layers of MoS_2 and WSe_2 [Marco M. Furchi et al, Nano Lett., vol14, p4785, 2014]. The researchers were able to tune the junction with a gate potential applied to the substrate, achieving photovoltaic charge transfer.

The substrate was silicon dioxide on silicon. The TMD layers were achieved using exfoliation from bulk crystals. The first TMD layer was exfoliated directly onto the substrate and then annealed in vacuum at 380K for several hours. The second TMD layer was transferred using PMMA at 380K.

The sample was then cooled to room temperature and the PMMA removed. The structure was finished with focused-ion beams used to cut away chunks of bulk material that would make short-circuits and with further annealing at 380K. Palladium was used as the contact metal.

Photoluminescence measurements on MoS_2 and WSe_2 monolayers gave peaks for A-excitons at 1.85eV and 1.65eV, respectively. The researchers estimate the exciton binding energy to be ~0.5eV, which added to the energies of the exciton resonances should give the bandgap energy. The MoS_2 PL spectrum also showed a 2.0eV B-exciton.

The gate potential affected the carrier characteristic of the WSe_2, changing from n-type (> −11V) to p-type (<-47V). By contrast, the MoS_2 layer is n-type down to full depletion at −71V. The n-type behavior of the MoS_2 layer is attributed to thermally activated impurity states that contribute electrons to the conduction band.

By biasing the gate between −71V and −47V, a pn junction is formed between the materials, giving diode current rectification.

The photovoltaic performance was measured with the gate potential −50V and a halogen lamp giving incident optical power between 180W/m^2 and 6400W/m^2. The researchers believe that excitons generated in the separate layers relax into interlayer exciton states due to the type-II heterostructure. The carriers then diffuse laterally to the contacts. The dominant efficiency limiting factor is interlayer recombination, the researchers believe. The researchers estimate an external quantum efficiency of 1.5% at 590nm wavelength. The power conversion efficiency of 0.2% is comparable to values obtained for bulk WSe_2 (0.1–0.6%) and MoS_2 (1%).

The researchers believe that stacking or plasmonic enhancement could result in better efficiency. With plasmonic enhancement of 10% and sandwiching the dichalcogenide junction between electrodes for vertical carrier extraction could give 5x better efficiency, says the team.

The researchers believe that "Bringing together different 2D materials in a roll-to-roll process or direct heterostructure growth could lead to a new photovoltaic solar technology. Moreover, due to the plurality of 2D materials with different band gaps and electron affinities, low-cost multijunction solar cells could come within reach."

One-dimensional heterojunctions

Researchers based in USA, UK, and Hong Kong have developed a physical vapor transport process that creates one-dimensional (1D) heterojunctions between 2D semiconductor monolayers of $MoSe_2$ and WSe_2 [Chunming Huang et al, Nat. Mater., published online 24 August 2014]. The team consisted of members

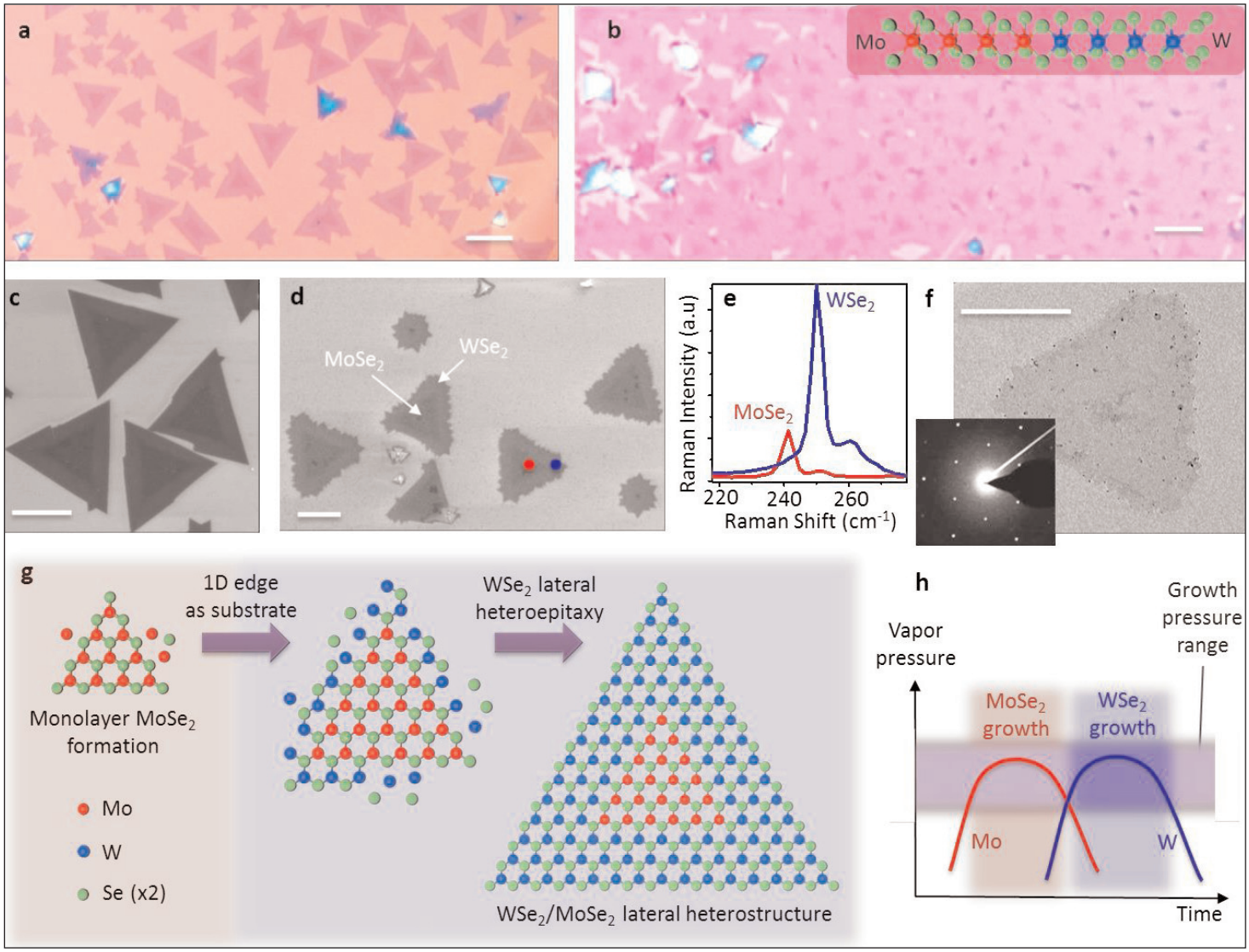

Figure 3. In-plane hetero-epitaxy of 2D $MoSe_2$/WSe_2 lateral heterostructures. a, Optical image of triangular heterostructure crystals. b, Optical image of semi-continuous film. Inset: side-view cartoon of in-plane heterojunction. c and d, SEM images of heterostructure crystals from two different growths. All scale bars 10μm. e, Raman spectra (514.5nm laser excitation) taken at points indicated in d. f, BF TEM image of isolated heterostructure. Inset shows electron diffraction pattern implying a single undistorted lattice. Scale bar: 5μm. g, Schematic illustration of process of in-plane epitaxial growth of lateral heterostructures. h, Schematic of atomic vapor pressure variation leading to growth of two materials in sequence.

from University of Washington, University of Warwick, and University of Hong Kong.

"Heterojunctions are fundamental elements of electronic and photonic devices," comments Xiaodong Xu, an assistant professor of materials science and engineering and of physics at University of Washington. "Our experimental demonstration of such junctions between two-dimensional materials should enable new kinds of transistors, LEDs, nanolasers, and solar cells to be developed for highly integrated electronic and optical circuits within a single atomic plane."

David Cobden, professor of physics at University of Washington adds: "In the future, combinations of two-dimensional materials may be integrated together in this way to form all kinds of interesting electronic structures such as in-plane quantum wells and quantum wires, superlattices, fully functioning transistors, and even complete electronic circuits."

The researchers quote the direct optical bandgaps of $MoSe_2$ and WSe_2 at 1.550eV and 1.653eV, respectively. The lattice constants of the two-dimensional materials are close to each other: 3.280Å for WSe_2 and 3.288Å for $MoSe_2$. The Washington/Warwick/Hong Kong team suggests that their horizontal $MoSe_2$/WSe_2 1D heterojunctions may also lead to type II behavior and thus efficient charge separation.

Growth of the lateral heterostructures was achieved through physical vapor transport from $MoSe_2$ and WSe_2 powders in hydrogen onto silica-on-silicon substrate in a 1-inch tube furnace. The sources were heated to 950ºC. The temperature in the substrate region of the tube was 650–750ºC.

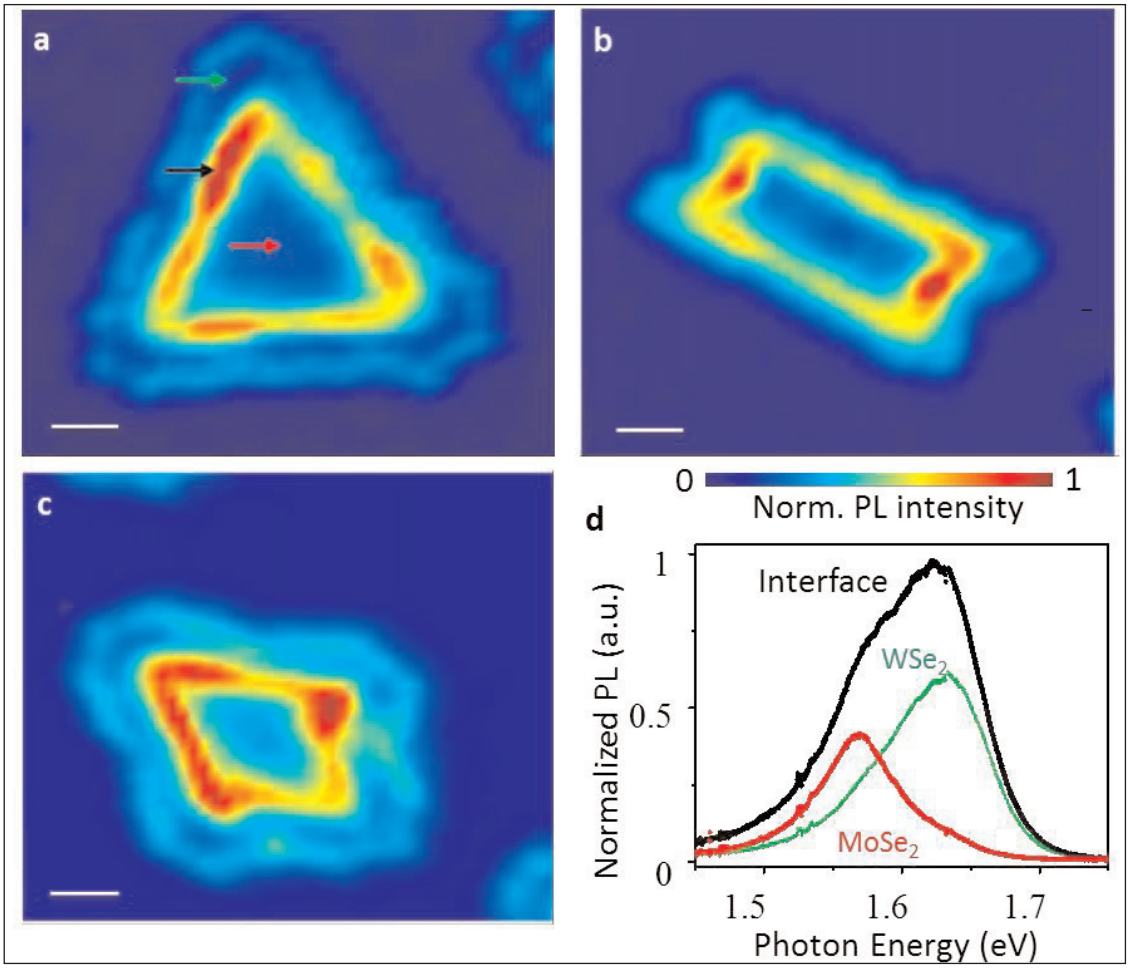

Figure 4. Photoluminescence from 1D heterointerfaces. a, 2D PL intensity map of triangular lateral heterostructure. Scanning micro-PL was performed with 532nm laser excitation at room temperature. b & c, Similar measurements for heterostructures with other shapes. Scale bars: 2μm. d, PL spectra taken at points indicated in a.

The researchers believe that a larger furnace would make it possible to mass-produce sheets of $MoSe_2/WSe_2$ semiconductor heterostructures. With the 1-inch tube furnace, it took about five minutes to grow the crystals. However, the heating and cooling took up to 2 hours.

The growth process often resulted in monolayer crystal patches of approximately equilateral triangles of side 15μm (Figure 3). Other shapes were also seen: strips, stars, arrows ... A wet process was used to transfer the monolayer material on PMMA to the analysis substrates (silicon dioxide, electron microscope grid, etc).

The triangular crystals tended to have darker inner regions and paler outer perimeters. Raman spectroscopy suggested that the inner regions tended to be $MoSe_2$ and the outer regions WSe_2. The researchers explain the structure as being due to $MoSe_2$ growth being favored early on but, as the vapor pressure shifts, the growth tips towards crystal WSe_2 monolayer coverage. The researchers add: "The similarity of the two materials permits the epitaxial growth of WSe_2 directly on existing $MoSe_2$ crystal edges."

The shift in growth from $MoSe_2$ to WSe_2 may also be due to the different evaporation properties of the source powders.

The researchers comment: "The reproducibility of our results suggests that a more sophisticated setup with independent control of the vapor components could be developed if necessary to create heterojunction sequences programmably for complex device applications."

Such sequences could be used to create one-dimensional quantum wells within the two-dimensional semiconductor monolayers.

Analysis with various techniques suggested that all the atoms lay on a single MX_2 honeycomb lattice with no dislocations or grain boundaries. The interface between the $MoSe_2$ and WSe_2 regions occurs on a scale of several lattice constants. In the interface region the material is an alloy of the two materials, i.e. $W_xMo_{1-x}Se_2$ with a steep x-composition gradient from 0 to 1. Away from the interface the researchers found some Mo substitutions on the WSe_2 side. Also, some Se vacancies were apparent.

Microscopic photoluminescence (PL) studies showed exciton peaks at 1.57eV and 1.63eV in the $MoSe_2$ and WSe_2 regions, respectively (Figure 4). These are 'identical' with the values found for homogeneous $MoSe_2$ and WSe_2 monolayers.

The peak for the heterojunction region was intermediate in energy and broader than for the pure $MoSe_2/WSe_2$ regions. Also, the emission was brighter — "possibly due to trapping of excitons by defects or enhanced radiative recombination at the interface".

As yet, no electron transport study has been made due to the lack of a suitable, reliable contact structure.

Contact technology

With the need for a better methodology in mind, Rutgers University and Los Alamos National Laboratory in the USA have developed a strategy for creating contacts in ultrathin MoS_2 nanosheets (2–3 layers) by

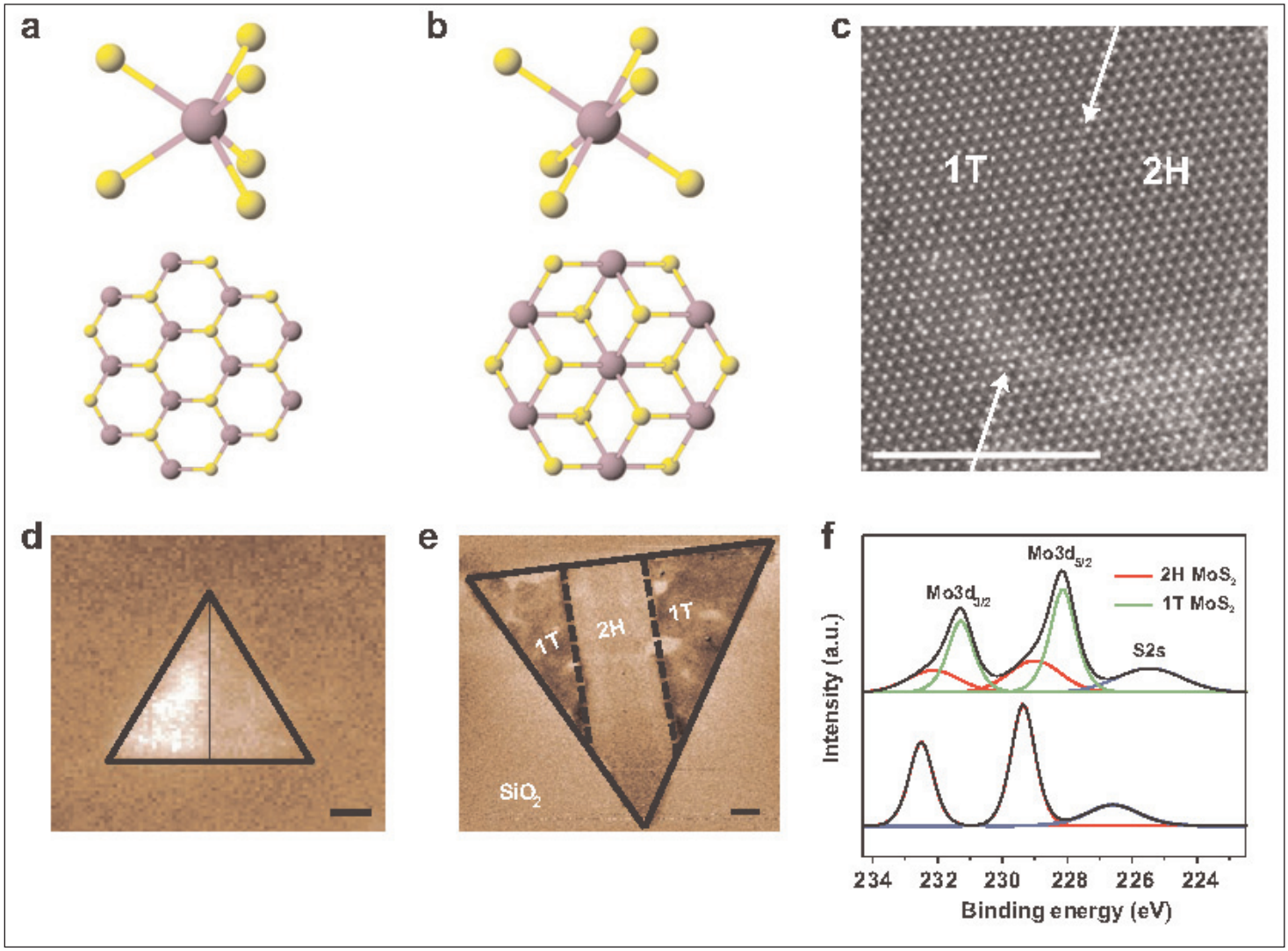

Figure 5. 1T and 2H phases of MoS_2. a,b, Crystal structures of 2H and 1T phases, respectively (purple, metal; yellow, chalcogen). c, High-resolution transmission electron microscope image of atomically thin phase boundary (indicated by arrows) between 1T and 2H phases in MoS_2 monolayer (scale bar 1nm). d, Photoluminescence map of triangular MoS_2 monolayer – left side 2H phase, right side converted to 1T. e, Electrostatic force microscopy phase image of MoS_2 monolayer (scale bars 1μm). f, X-ray photoelectron spectra (XPS) showing Mo3d and S2s peaks of 1T and 2H phases of MoS_2. Typical experimentally measured spectra are shown in black and fits are shown in red (for 2H phase) and green (for 1T phase). The lower curve is 100% 2H phase, whereas the top curve can be fitted with both 1T and 2H phase components.

locally transforming the phase from the semiconducting 2H to metal 1T crystal structure [Rajesh Kappera et al, Nature Materials, published online 31 August 2014]. A contact resistance of 200–300Ω-μm (0.2–0.3kΩ-μm) was achieved at zero gate bias in a field-effect transistor structure. The resistance was reduced a further factor of three with +30V gate potential.

These contact resistances represent a five-fold improvement over values for 2H MoS_2 contacts that are in the range ~1kΩ-μm. "The 1T contact resistance values are lower than the best values of ~0.6–0.7kΩ-μm reported thus far for MoS_2 devices," the researchers add. The 1T contact resistance is even comparable with state-of-the-art for metal/silicon (0.3–0.5kΩ-μm), as reported in the 2012 International Technology Roadmap for Semiconductors.

The researchers comment: "The low contact resistance is attributed to the atomically sharp interface between the phases and to the fact the work function of the 1T phase and the conduction band energy relative to vacuum level of the 2H phase are similar (~4.2eV)." The transistors demonstrated ~50cm^2/V-s effective mobility, 85μA/μm drive current, 90–100mV/decade subthreshold swing, and ~10^7 on/off current ratio. The researchers also found the device performance of 1T electrodes to be highly reproducible and independent of the contact metal (gold, calcium, palladium).

The MoS_2 was exfoliated onto SiO_2/Si substrates. The MoS_2 flakes were covered with PMMA and openings made for the contact regions by photolithography. The transformation to 1T polytype (Figure 1) was achieved by treatment with n-butyl lithium at room temperature

for 1 hour. After treatment, residues were washed away with hexane and de-ionized water. The 1T regions were found to have a phase concentration of 70%. The researchers expect even better transistor performance if this concentration were to be increased.

Device fabrication continued with application of metal pads to the contact areas. The gate structures were also produced at the same time in top and bottom configurations. High-k dielectrics for the top-gate configuration were deposited in atomic layer deposition (hafnium dioxide) or plasma-enhance chemical vapor deposition (silicon nitride) processes.

The team comments: "The 1T phase is metastable, but we have demonstrated that it is stable under environmental conditions and also as catalyst for hydrogen evolution — however, its stability under high-performance device operation remains to be elucidated."

Although we have focused on compounds with S/Se, another possibility for the chalcogenide is tellurium (Te). University of Geneva researchers have found a direct bandgap of 1.02eV and a narrower indirect bandgap of 0.88eV for 4nm-thick $MoTe_2$ crystals [Ignacio Gutiérrez Lezama et al, 2D Mater., vol1, p021002, 2014]. The researchers are hopeful that there will be a transition to a direct bandgap when thinner layers are studied.

Other researchers have studied the coupling with polarized light and have been able to generate and manipulate spin and valley currents [Tao Jiang et al, Nature Nanotechnology, published online 31 August 2014, Fudan University, Collaborative Innovation Center of Advanced Microstructures, University of California at Berkeley; Hongtao Yuan et al, Nature Nanotechnology, Published online 7 September 2014, Stanford University, SLAC National Accelerator Laboratory, Peking University, Collaborative Innovation Centre of Quantum Matter].

The spin current is related to the magnetic moment of the electron, while a valley current consists of electrons in a particular part of the band structure. The distinct valleys in the band structure can be theoretically treated as an index with a similar influence on electron dynamics as spin. While 'spintronics' has been researched for some time, the possibility of 'valleytronics' has only been discussed recently in the context of graphene and TMDs. ■

Author:
Mike Cooke is a freelance technology journalist who has worked in the semiconductor and advanced technology sectors since 1997.